



Contents lists available at SciVerse ScienceDirect

Tetrahedron

journal homepage: www.elsevier.com/locate/tet



Synthesis and structural study of 2-arylbenzotriazoles related to Tinuvin

Dolores Santa María^a, Rosa M. Claramunt^{a,*}, Vladimir Bobosik^b, M. Carmen Torralba^c, M. Rosario Torres^{c,*}, Ibon Alkorta^d, José Elguero^d

^aDepartamento de Química Orgánica y Bio-Orgánica, Facultad de Ciencias, Universidad Nacional de Educación a Distancia (UNED), Senda del Rey 9, E-28040 Madrid, Spain

^bSynkova, Mlynská dolina, Areál PvF UK, SK-84215 Bratislava, Slovak Republic

^cDepartamento de Química Inorgánica I and CAI de Difracción de Rayos-X, Facultad de Ciencias Químicas, Universidad Complutense de Madrid (UCM), E-28040 Madrid, Spain

^dInstituto de Química Médica, Centro de Química Orgánica "Manuel Lora-Tamayo", CSIC, Juan de la Cierva 3, E-28006 Madrid, Spain

ARTICLE INFO

Article history:

Received 9 November 2012

Received in revised form 17 January 2013

Accepted 31 January 2013

Available online xxx

Dedicated to our friend and pioneer of this class of compounds John F. K. Wilshire

ABSTRACT

A total number of nineteen 2-arylbenzotriazoles related to the UV absorber Tinuvin P have been studied. Moreover, besides those bearing a 2'-hydroxy substituent, known to experience ESIPT (Excited-State Intramolecular Proton Transfer), we have also prepared three compounds having another *ortho*-hydroxy group at position 6'. The X-ray molecular structures of five key representatives have been determined and some important features related to their behavior discussed on the basis of solution and solid-state NMR, as well as B3LYP/6-311++G(d,p) computational results.

© 2013 Elsevier Ltd. All rights reserved.

1. Introduction

There are two main classes of UV absorbers, the 2-hydroxyarylbenzotriazoles of Ciba (Tinuvin)¹ and the 2,4,6-triaryl-1,3,5-triazines of BASF (Tinosorb S) (note that since Ciba and BASF merged in April 2009 both photoprotectors now belong to BASF).² They find application in many domains, one very active and economically very profitable, as in polymers and 'sun care' products. The photophysics of Tinuvin and related compounds has been extensively studied,³ included by us.⁴

The protection mechanism is based on the so-called ESIPT (Excited State Intramolecular Proton Transfer) that we illustrated in Fig. 1 for Tinuvin P. Ultraviolet absorbers, such as Tinuvin P achieve their exceptional photostabilities as a result of deactivation of excited singlet states through excited state intramolecular proton transfer (ESIPT).⁵

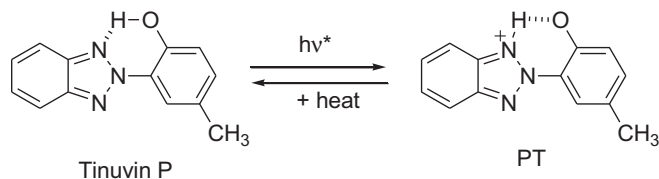


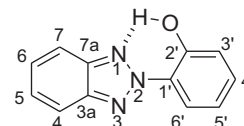
Fig. 1. The ESIPT mechanism.

* Corresponding author. E-mail address: rclaramunt@ccia.uned.es (R.M. Claramunt).

In the present paper we will report our studies about the structure of Tinuvin P (drometrizole) and other Tinuvin [320 (UV-320), 326 (bumetrizole), and 327] as well as other literature compounds (Fig. 2). All these compounds, save **19**, have one (**1–15**) or two *ortho*-hydroxy groups (**16–18**). Besides Tinuvin **1–4**, the known compounds of Fig. 2 are reported in the following papers: **5**,^{5a} **6**,^{5a} **7**,⁶ **8**,⁶ **9**,⁶ **10**,^{6–8} **11**,⁶ **12**,^{6,8,9} **13**,^{8,10} **14**,¹⁰ **16**,⁷ **18**,^{6,11} and **19**.⁷

Compounds **16–18** were designed for future studies of the ESIPT mechanism (Fig. 3). The second hydrogen bond (HB) in PT1 should favor the planar structure. A second proton transfer to afford PT2 seems highly improbable.

The nomenclature used in the text and in the experimental is not in accordance with IUPAC rules. For all of the compounds with phenolic hydroxyl groups, the phenol system has the highest priority; however, using IUPAC nomenclature here would be at the expense of comparability and clearness. For instance, compound **18** would be 2-(2*H*-benzo[*d*][1,2,3]triazol-2-yl)-4,6-di-*tert*-butylbenzene-1,3-diol under IUPAC rules, rather than 2-(2,6-dihydroxy-3,5-di-*tert*-butylphenyl)-2*H*-benzotriazole. In order to prioritize comparability over correct nomenclature, we have named all of the compounds as 2*H*-benzotriazole derivatives.



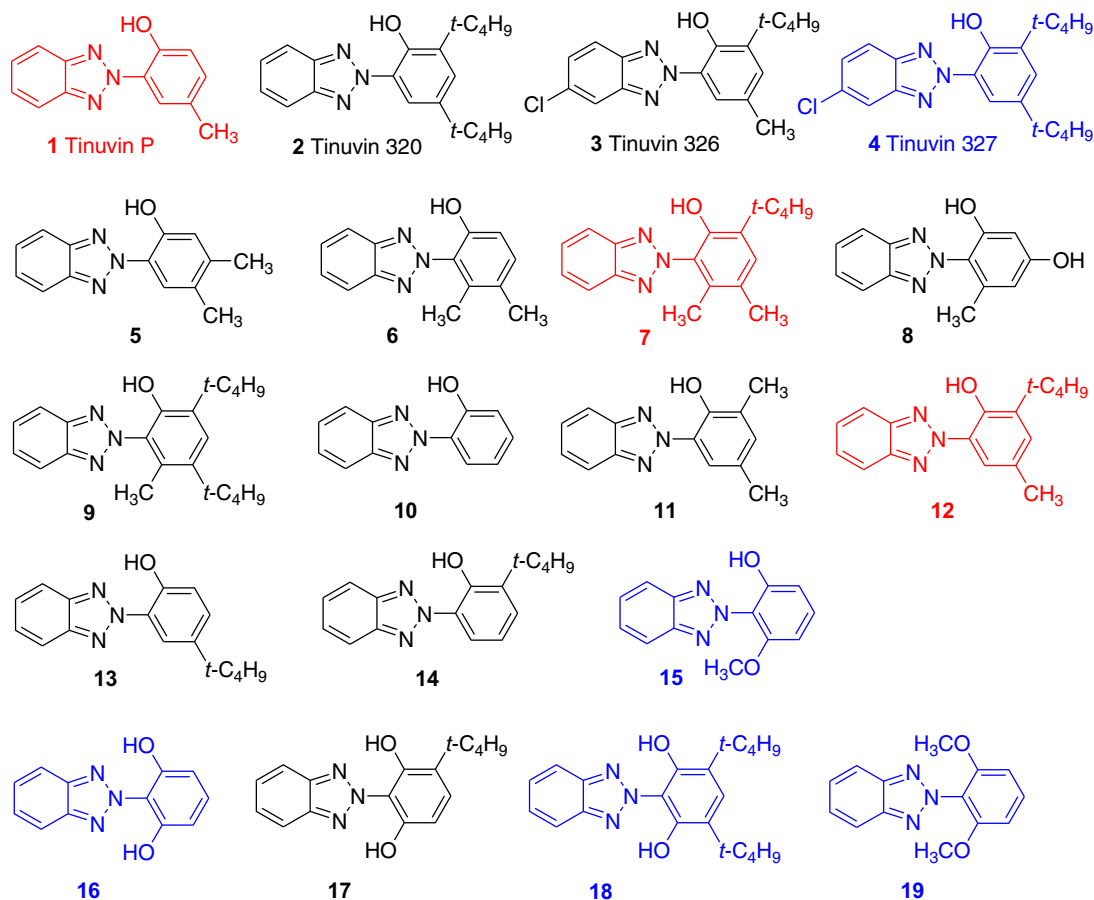


Fig. 2. Tinuvin and related molecules. In red, X-ray structures already known. In blue structures determined in the present work.

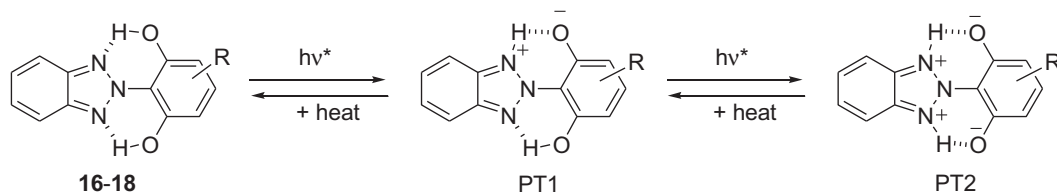


Fig. 3. Possible ESIPT mechanism for compounds 16–18.

The structural characterization of these compounds is scarce. ^1H , ^{13}C , and ^{15}N NMR data were reported for **1**,^{4d} but only ^1H NMR for **5**,^{5a} **6**,^{5a} and **12**.⁹ A search in the Cambridge Structural Data base (CSD)¹² reveals that the X-ray structures of Tinuvin P (**1**, refcode NIQDOG)^{4b,13} and of **12** (refcode KUCBUF) were twice determined.^{6,10} Surprisingly that of **7** was also determined by Rieker et al.⁶ but not reported in the CSD. One of the most interesting results from the X-ray determinations is the torsion angle about the phenyl and the 2*H*-benzotriazolyl rings as defined by N1–N2–C1'–C2': 1.4° (**1**), 89.3° (**7**), 5.3° (**12**). In compounds **1** and **12** there is an O–H···N1 intramolecular hydrogen-bond (IMHB) that is absent in **7**.

2. Results and discussion

2.1. Synthesis of benzotriazoles **15**, **16**, **17**, and **18**

Compound **18** was known and its synthesis started from 2-nitroaniline through the azo derivative **24**.¹¹ The procedure we report here, inspired in *tert*-butylation of phenols using inorganic supports,¹⁴ is simpler and more efficient. Fig. 4 summarizes the overall synthetic pathways.

The 2-substituted benzotriazole **19** was prepared using the thermal decomposition of the 5-(2,4-dimethoxyphenyl)-1-(2-

nitrophenyl)-1*H*-tetrazole (**21**) via a 2-nitrodiphenylcarbodiimide intermediate,¹⁵ a method that we had successfully applied to other cases.^{4c,d} The tetrazole was in turn formed by heating the corresponding 2'-nitrobenzanilide (**20**) in toluene containing phosphorous pentachloride to give *N*-(2-nitrophenyl)benzimidoyl chloride, which was then treated with sodium azide in dry *N,N'*-dimethylformamide.

Demethylation of **19** yields 2,6-dihydroxy-2*H*-benzotriazole (**16**), which under monomethylation affords **15**.

tert-Butylation of **16** permitted, by varying the reaction conditions, to obtain derivatives **17** and **18** as shown in the Experimental section.

2.2. X-ray structure determination of compounds **4**, **15**, **16**, **18**, and **19**

Tinuvin 327, compound **4**, was crystallized from chloroform/ethanol. Crystals of **15**, **16**, and **19** were obtained by slow evaporation of a chloroform solution, and those of **18** from chloroform/hexane. The bond distances and angles of the hydrogen bonds for compounds **4**, **15**, **16**, and **18** are summarized in Table 1.

Compound **4** crystallizes in the triclinic *P*-1 space group with one molecule per asymmetric unit (Fig. 5). The molecule is not completely planar, the dihedral angle between the least-squared

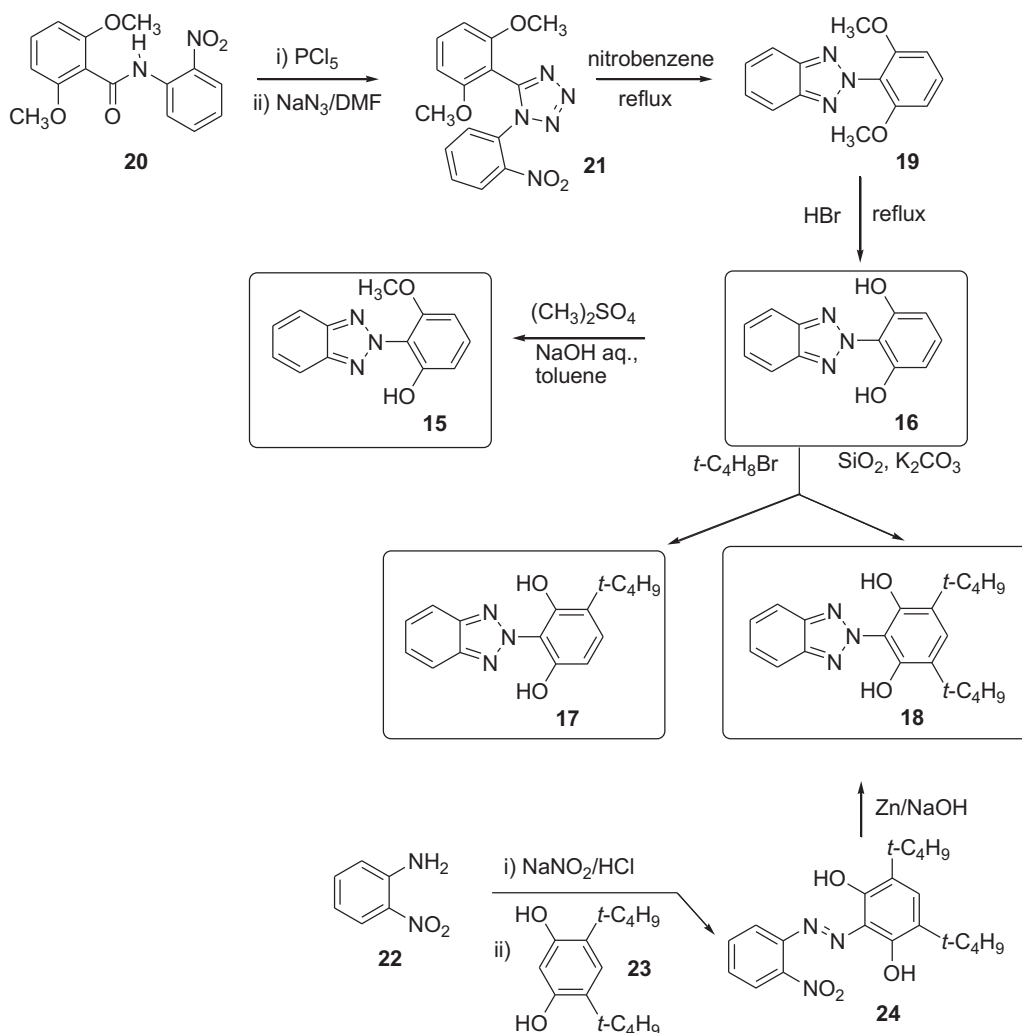


Fig. 4. Synthetic procedures followed to prepare compounds 15, 16, 17, and 18.

Table 1
Hydrogen bonds (Å and °) for compounds 4, 15, 16, and 18

Compound	D–H⋯A	Symmetry operations	d(D–H)	d(H⋯A)	d(D⋯A)	<(DHA)
4	O1–H1⋯N1		1.09	1.57	2.593(3)	153.9(1)
15	O1–H1⋯O3	$x, -y+1/2, z$	1.01	1.66	2.664(2)	177.3(1)
15	O3–H3A⋯N1'	$-x, -y, -z$	0.98	1.94	2.915(2)	172.0(1)
16	O1–H1⋯N1	$x, -y+1/2, z$	1.07	1.82	2.603(3)	126.5(1)
18	O1–H1⋯N1	$x, -y+1/2, z$	1.08	1.55	2.559(3)	152.6(1)
18	O2–H2⋯N3		1.04	1.61	2.543(3)	146.3(1)

planes that contain the benzotriazole fragment and the phenyl ring being of $12.7(1)^\circ$. The bond distances of the benzotriazole moiety present an extended electronic delocalization confirmed by its planarity. The hydroxyl group shows some positional disorder between C9 (O1 with 80% occupancy) and C13 (O1' with 20% occupancy). For this reason, the molecule presents intramolecular hydrogen bonds O1⋯N1 and O1'⋯N3 that might favor a major planarity of the molecule.

Compound 15 crystallizes in the orthorhombic system, space group $Pnma$. The asymmetric unit corresponds to half arylbenzotriazole molecule and half crystallization water molecule (Fig. 6), the planar hydroxymethoxyphenyl group is located on the mirror plane, with the planar benzotriazole moiety set perpendicularly.

The different molecules interact through the crystallization water molecules with formation of intermolecular hydrogen bonds

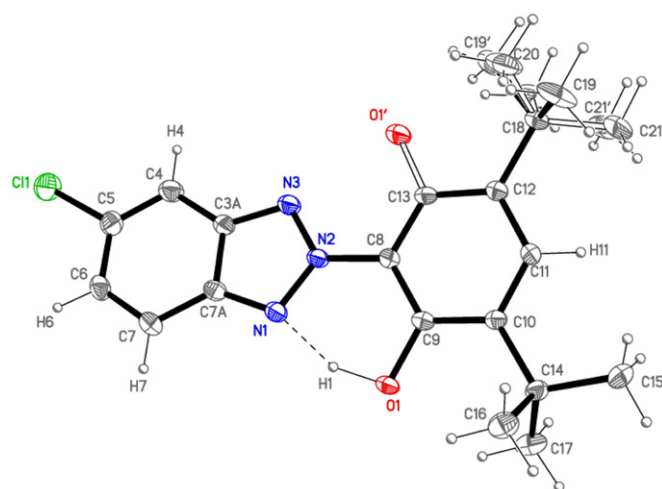


Fig. 5. ORTEP plot (20% probability for the ellipsoids) of 4, showing the labeling scheme. The white bonds correspond to the 20% occupancy of the disordered hydroxyl and the 37% of the *tert*-butyl groups.

O1–H1A⋯O3–H3A⋯N1'. In this way, each water molecule forms three intermolecular hydrogen bonds with three different molecules, one interaction through the hydroxyl group and the other two with the N1 atoms giving rise to a chain along *b*-axis (Fig. 7).

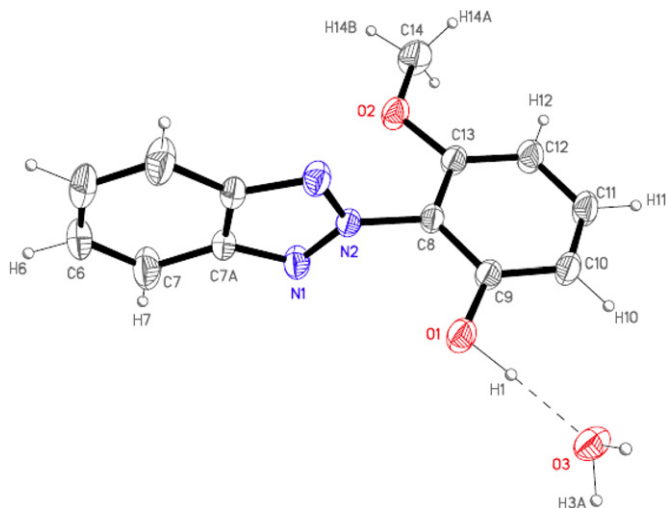


Fig. 6. ORTEP plot (20% probability) of **15**, showing the labeling of the asymmetric unit.

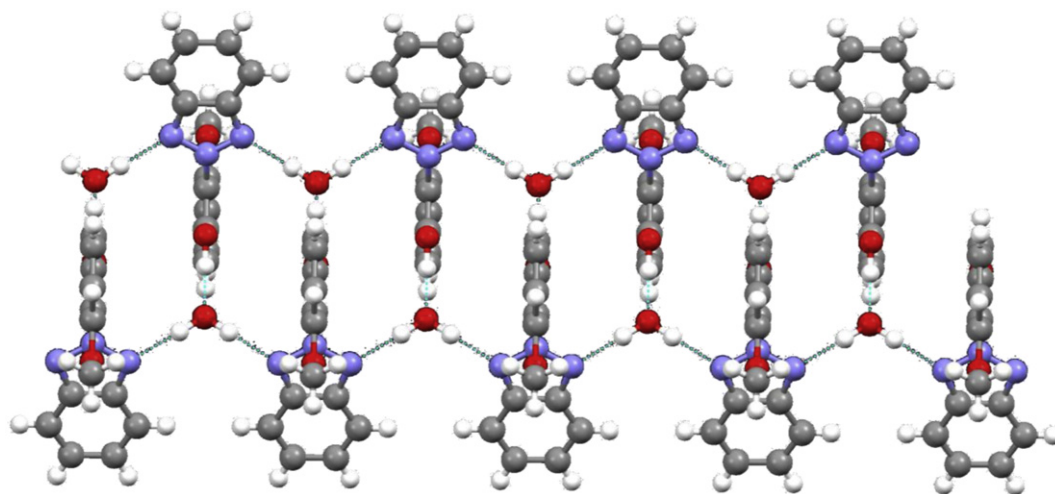


Fig. 7. View of the crystal packing of **15** showing the chain formed by intermolecular H-bonds along the *b*-axis.

The derivative **16** also crystallizes in the *Pnma* orthorhombic space group with half molecule per asymmetric unit. In this case, the molecule is perpendicular to the mirror plane that passes through N2, C8, and C11 (Fig. 8). The benzotriazole and dihydroxyphenyl rings are planar since both halves are related by the reflection in the symmetry plane, however, the molecule is not completely planar having a dihedral angle between the rings of

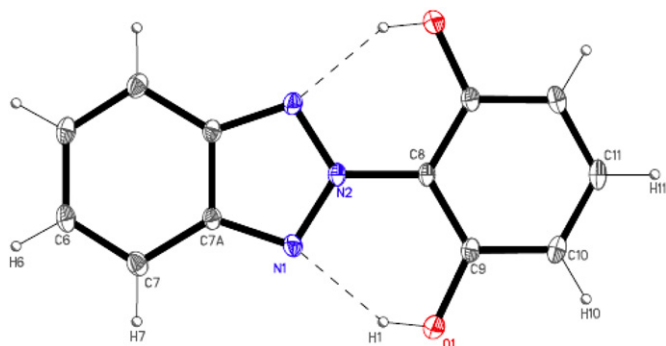


Fig. 8. ORTEP plot (20% probability) of **16**, showing the labeling of the asymmetric unit. Dotted lines indicate the intramolecular hydrogen bonds.

4.4(1)°. The hydroxyl groups form 2 equiv intramolecular hydrogen bonds O1–H1···N1.

The crystal structure of **18** (monoclinic *P2₁/m* space group) consists of planar molecules since all the atoms, except C19 and C16, and 16 H atoms of the methyl groups, are located on the symmetry plane (Fig. 9). As in the previous structure, the hydroxyl groups form two intramolecular hydrogen bonds O1–H1···N1 and O2–H2···N3.

The compound **19** crystallizes in the orthorhombic *Iba2* space group with two molecules displayed almost perpendicularly in the asymmetric unit. Both molecules are chemically equivalent but crystallographically independent. In each molecule the benzotriazole moiety and the dimethoxyphenyl group are perpendicular with dihedral angles of 86.5(1)° for molecule 1 and 86.6(1)° for molecule 2 (Fig. 10). The bond distances and angles indicate that both molecules are very similar, the main difference between them being the relative positions of methyl groups, which are almost coplanar with the phenyl ring in molecule 1 but shifted out of the plane in molecule 2.

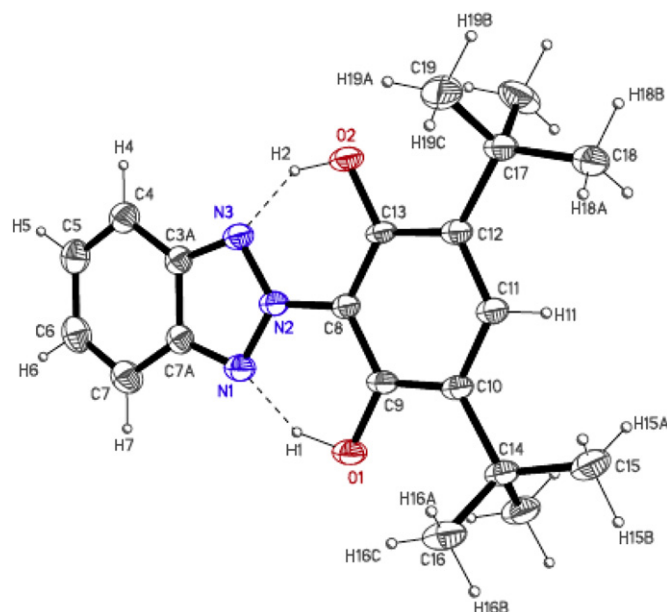


Fig. 9. ORTEP plot (20% probability) of **18**, showing the labeling of the asymmetric unit. Dotted lines indicate the intramolecular hydrogen bonds.

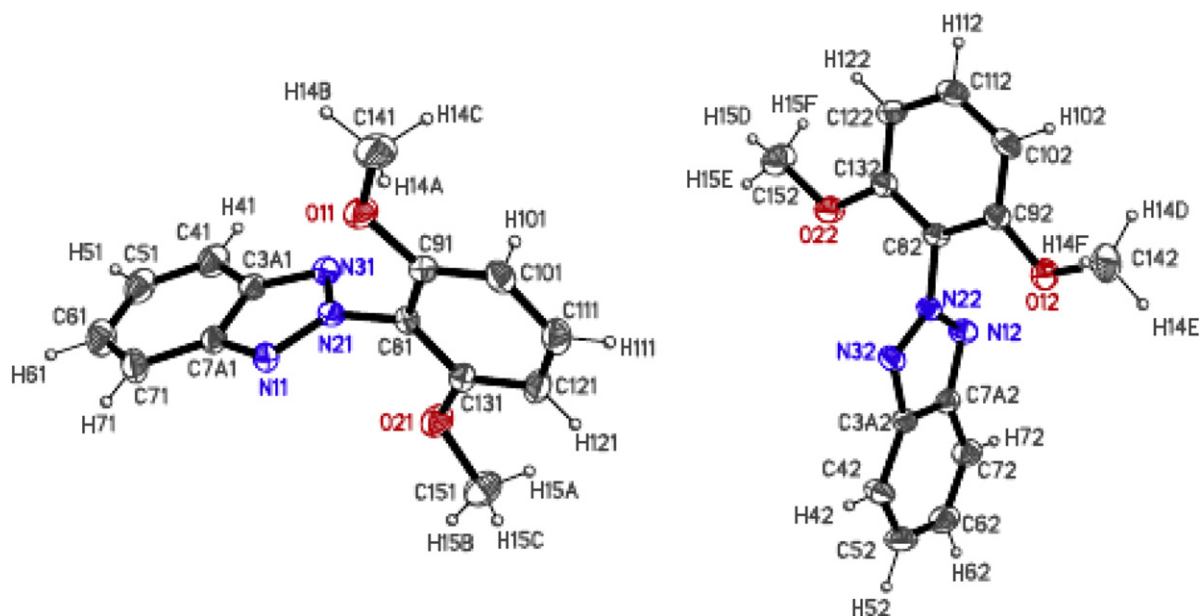


Fig. 10. ORTEP plot (30% probability) of **19**, showing the labeling of the two molecules that form the asymmetric unit.

A comparison among the five crystal structures reported leads to the following remarks:

In all compounds the benzotriazole fragment is planar exhibiting an extended electronic delocalization. The bond distance N2–C8 of about 1.43 Å is very similar for **15**, **16**, **18**, and **19**, but it is a bit shorter, 1.423(3) Å, in **4**. In this latter case such shortening can be explained as due to the steric effect of the chlorine atom on the crystalline packing.

The main differences observed are related to the coplanarity between the benzotriazole and the phenyl rings. This coplanarity appears when two intramolecular H-bonds between the hydroxyl groups and the triazole fragment are formed, as found in **16** and **18**. On the contrary, when no intramolecular hydrogen bonds are formed, derivatives **15** and **19**, the two moieties of the molecule tend to be perpendicular. Finally, compound **4** shows an intermediate situation with formation of only one intramolecular H-bond leading to a torsion angle between both fragments of 12.7°. This fact would indicate that the more stable conformation, due to lower steric hindrance, is the perpendicular one. The formation of intramolecular hydrogen bonds compensates the loss in stability when the molecule adopts the planar conformation.

The presence of additional substituents in the phenyl ring does not affect the conformation of the molecule.

2.3. NMR studies

The results concerning the ^{15}N and ^{13}C NMR in solution as well as in the solid state are given in Tables 2 and 3, respectively. ^1H NMR data in solution can be found in the electronic Supplementary data (ESI). All assignments have been made taking into account the multiplicity of the signals and 2D correlation experiments: (^1H – ^1H) gs-COSY, (^1H – ^{13}C) gs-HMQC, (^1H – ^{13}C) gs-HMBC, and (^1H – ^{15}N) gs-HMBC;

those of N2 were obtained using the inverse gated ^1H decoupling technique.

those of N2 were obtained using the inverse gated ^1H decoupling technique.

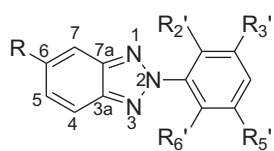
In solution, the rotation about the N2–C1' bond is fast in the NMR time scale, consequently the chemical shifts of N1 and N3 are average (Table 2), an average that disappears in the solid state (Table 3). For compounds **3** and **4**, although averaged, the signals are different due to the effect of the chlorine atom. In Fig. 11 is presented the 2D (^1H – ^{15}N) correlation experiment for compound **3** Tinuvin 326.

Using the ^{13}C chemical shifts in solution we have estimated the degree of interannular conjugation. As shown in Fig. 12, we have first determined the effects of the OH substituent from the experimental data of Tinuvin P (**1**) and of 2-phenylbenzotriazole,^{4d} taking those of the methyl group of **1** from the Kalinowski's book (CH₃: Z₁ 9.2, Z₂ 0.7, Z₃ –0.1, Z₄ –3.1).¹⁶ Then, we have also calculated those of the *t*-Bu group, and with these increments and those of the OCH₃ group (Z₁ 31.4, Z₂ –14.4, Z₃ 1.0, Z₄ –7.7),¹⁶ the values gathered in Table 4 were obtained.

For the solid state the conclusions were the same although there are small differences in the $\delta_{\text{C-meta}} - \delta_{\text{C-ortho}}$ values: 10.8 (**PhBzTr**), 8.9 (**1**), 8.6 (**3**), 11.4 (**4**), 11.3 (**16**), 9.0 (**17**), 7.9 (**18**), and 3.2 (**19**). The splitting of several signals in compound **19** corresponds to the presence of two independent molecules in the unit cell (Fig. 10). In the case of compound **4** the splitting of the NMR signals are due to the existence of two atropisomers around the N2–C1' bond, and from the intensities of the ^{15}N NMR signals in solid state for N2 and N3 (Table 3) the estimated proportions of both isomers are in agreement with the values obtained from the X-ray diffraction studies (Fig. 5).

2.4. Computational results

We have calculated the geometries of all the compounds of Fig. 2 and reported the results in Table 5. In the case of compounds **3** and **4**, due to the presence of the chlorine atom, there are two conformations (Fig. 13) that differ only in 0.08 kJ mol^{–1}. However, their dipole moments are quite different, being twice for conformers **3** and **4** than for conformers **3'** and **4'**.

Table 2
¹⁵N and ¹³C NMR chemical shifts (δ in ppm) of 2H-benzotriazoles **3**, **4**, **15**–**19** in CDCl₃ at 40 and 100 MHz, respectively. ¹H–¹³C coupling constants (*J* in Hz) are given in the ESI

- 3**, R = Cl, R_{2'} = OH, R_{6'} = H, R_{3'} = *t*-C₄H₉, R_{5'} = CH₃
4, R = Cl, R_{2'} = OH, R_{6'} = H, R_{3'} = R_{5'} = *t*-C₄H₉
15, R = H, R_{2'} = OH, R_{6'} = OCH₃, R_{3'} = R_{5'} = H
16, R = H, R_{2'} = R_{6'} = OH, R_{3'} = R_{5'} = H
17, R = H, R_{2'} = R_{6'} = OH, R_{3'} = *t*-C₄H₉, R_{5'} = H
18, R = H, R_{2'} = R_{6'} = OH, R_{3'} = R_{5'} = *t*-C₄H₉
19, R = H, R_{2'} = R_{6'} = OCH₃, R_{3'} = R_{5'} = H

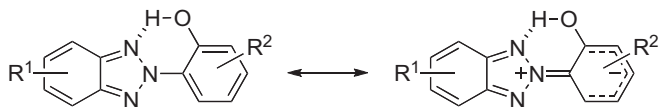
Comp.	3	4	15	16	17	18	19
N1	–78.9/–80.9	–78.6/–80.8	–65.5	–87.7	–87.8	–87.5	–58.8
N2	–106.6	–105.8	n.d.	–110.9	–109.9	–109.2	–124.6
N3	–78.9/–80.9	–78.6/–80.8	–65.5	–87.7	–87.8	–87.5	–58.8
C3a	141.1	141.1	143.9	140.3	140.2	140.0	144.5
C4	118.6	118.7	118.1	116.8	116.8	116.7	118.3
C5	129.0	129.0	127.4	128.3	128.3	128.1	126.4
C6	133.3 (Cl)	133.3(Cl)	127.4	128.3	128.3	128.1	126.4
C7	116.5	116.6	118.1	116.8	116.8	116.7	118.3
C7a	142.9	142.9	143.9	140.3	140.2	140.0	144.5
C1'	125.2	125.0	117.8	113.5	114.0	114.7	119.2
C2'	146.8 (OH)	146.7 (OH)	151.9 (OH)	150.8 (OH)	149.0 (OH)	147.6 (OH)	156.1 (OMe)
C3'	139.2 (^t Bu)	138.7 (^t Bu)	110.4	109.2	129.2 (^t Bu)	127.2 (^t Bu)	104.0
C4'	129.1	125.5	130.9	130.6	128.1	126.0	131.5
C5'	128.4 (Me)	141.8 (^t Bu)	104.2	109.2	107.7	127.2 (^t Bu)	104.0
C6'	119.4	116.2	154.0 (OMe)	150.8 (OH)	149.7 (OH)	147.6 (OH)	156.1 (OMe)
Subs.	35.4 (^t Bu) 29.5 (^t Bu) 20.9 (Me)	35.7 (^t Bu-3) 29.6 (^t Bu-3) 34.6 (^t Bu-5) 31.5 (^t Bu-5)	56.6 (OMe)	—	34.8 (^t Bu) 29.6 (^t Bu)	35.1 (^t Bu) 29.8 (^t Bu)	56.0(OMe)

Table 3
¹⁵N and ¹³C NMR chemical shifts (δ in ppm) of 2H-benzotriazoles **3**, **4**, **16**–**19** in the solid state at 40 and 100 MHz, respectively

Comp.	3	4	16	17	18	19
N1	–87.6	–86.7	–89.6	–89.2	–90.0	–53.0/–52.4
N2	–105.1	–103.4/–104.2	–106.5	–107.1	–108.9	–118.9
N3	–67.9	–66.5/–68.2	–89.6	–89.2	–90.0	–54.6/–53.9
C3a	141.6	140.0	137.6	137.6	136.8	144.9
C4	116.9	118.3	115.8	115.0	113.9	118.4
C5	129.1	130.7	128.6	128.0	127.3	128.5 ^a
C6	134.5 (Cl)	135.1 (Cl)	128.6	128.0	127.3	128.1 ^a
C7	115.2	115.5	115.8	115.0	113.9	117.4
C7a	141.6	142.6	137.6	137.6	136.8	144.9
C1'	124.5	124.1	111.3	113.4	113.9	119.0
C2'	146.5 (OH)	145.5 (OH)	150.2 (OH)	148.9 (OH)	148.2 (OH)	155.3 (OMe)
C3'	138.6 (^t Bu)	137.4 (^t Bu)	110.3	128.0 (^t Bu)	125.9 (^t Bu)	104.4 ^b
C4'	129.1	127.9	130.4	129.9	124.4	132.6
C5'	127.2 (Me)	140.0 (^t Bu)	110.3	108.7	127.3 (^t Bu)	104.7 ^b
C6'	120.1	115.5	150.2 (OH)	150.4 (OH)	148.2 (OH)	156.5 (OMe)
Subs.	36.0/29.8 (^t Bu) 18.6 (Me)	35.3/30.5 (^t Bu-3) 34.6/32.6 (^t Bu-5)	—	35.6/29.8 (^t Bu)	35.6/ 29.8&31.2 (^t Bu)	54.8 ^c (OMe-3) 56.9 ^c (OMe-5)

^a The assignment of these signals can be exchanged.^b The assignment of these signals can be exchanged.^c The assignment of these signals can be exchanged.

The interring C–N bond length is almost constant although it was expected to be shorter in planar structures due to N⁺=C resonance forms.



This is not the case, but the shorter distance corresponds to compound **4** (1.423 Å, $\theta=12.7^\circ$) and the longest to compound **7** (1.437 Å, $\theta=89.3^\circ$). Concerning DIC, if one quantify Ext=2, Med=1, Hin=0, then there is some relationship between DIC and θ ($R^2=0.84$).

The last three columns of Table 6 report the geometry of the IMHB. The number of IMHB indicates their possible existence even when due to the torsion they are weak or non-existent (compound **7**). In the X-ray structure of this compound ($\theta=89.3^\circ$) there is no

intramolecular O–H...N1 HB (even weak) but an intermolecular one. This explains why the calculated value (40.0°) is much lower than the experimental one. There is a good qualitative agreement with the DIC conclusions of Table 4.

We have calculated at the GIAO/B3LYP/6-311++G(d,p) level all the absolute shieldings (σ , ppm) of 2-phenylbenzotriazole (**PhBzTr**) and *ortho*-hydroxy derivatives **1**–**18** (Table 7). We have transformed these σ values into chemical shifts (δ , ppm) using empirical relationships we have established from large collection of data (see Supplementary data). As usual, the agreement is good with the experimental results and will no longer commented save for some selected examples.

Some interesting correlations were found between the experimental and calculated data:

Eq. 1 (that includes three literature values also determined in CDCl₃) indicates that the calculations reproduce well the

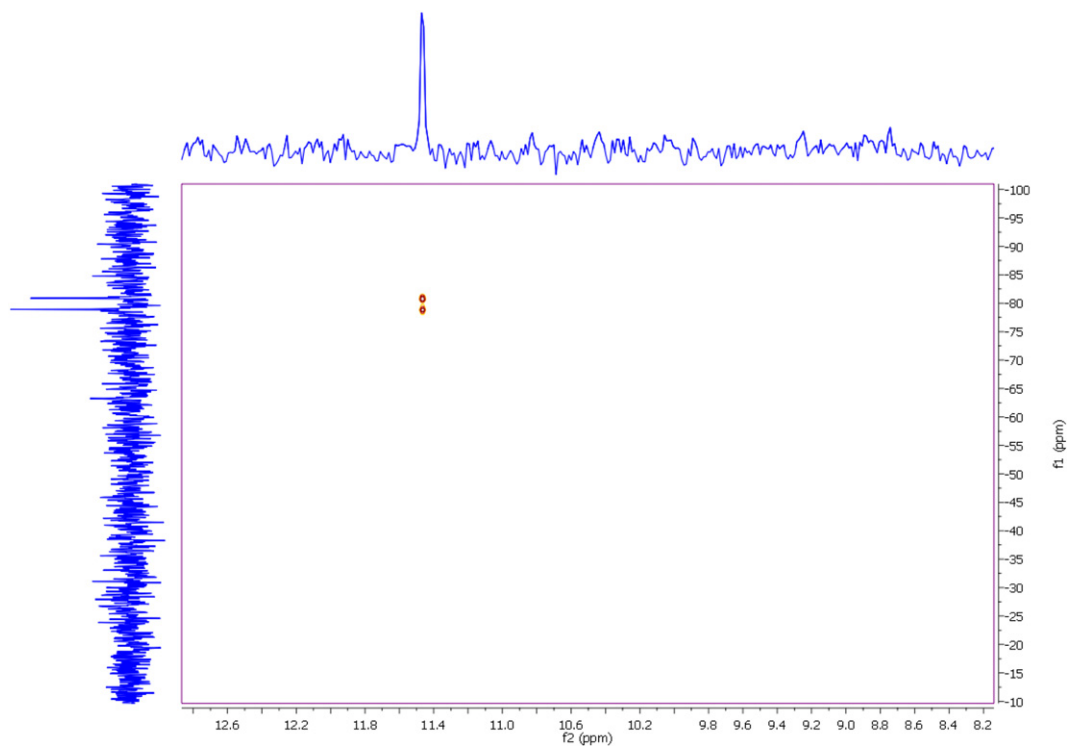


Fig. 11. 2D ($^1\text{H}-^{15}\text{N}$) gs-HMBC spectrum of **3** in CDCl_3 .

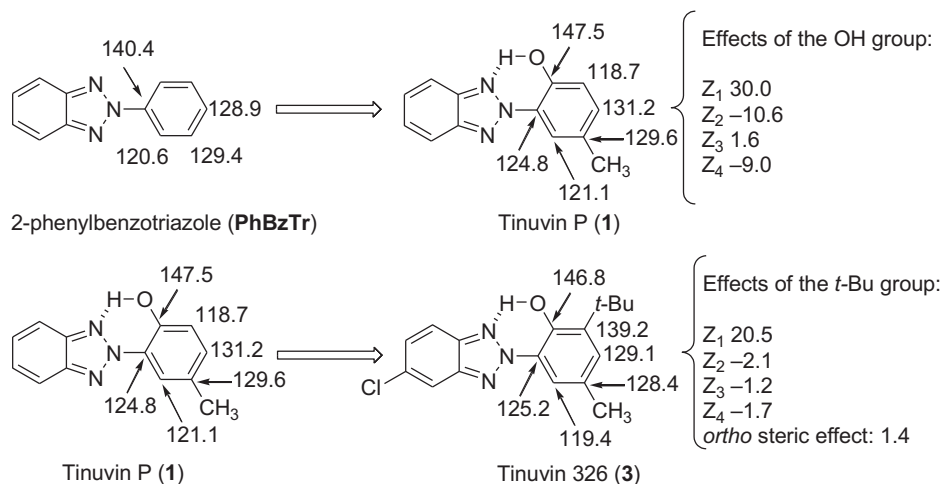


Fig. 12. Calculation of the additive effects of the OH and *t*-Bu groups.

Table 4

Estimation of the degree of interannular conjugation (DIC): extensive (Ext), medium (Med), hindered (Hin). Aver: average values (all in ppm)

Compound	$\delta_{\text{C-ortho}}$	$\delta_{\text{C-ortho}}$ Aver	$\delta_{\text{C-meta}}$	$\delta_{\text{C-meta}}$ Aver	$\Delta\delta = \delta_{\text{C-meta}} - \delta_{\text{C-ortho}}$	DIC
PhBzTr	120.6	120.6	129.4	129.4	8.8	Ext
1	147.5 - 30.0 + 3.1 = 120.6	119.7	118.7 + 10.6 + 0.1 = 129.4	129.4	9.7	Ext
	121.1 - 1.6 - 0.7 = 118.8		129.6 - 9.2 + 9.0 = 129.4			
3	146.8 - 30.0 + (2.1 - 1.4) + 3.1 = 120.6	119.7	139.2 - 20.5 + 10.6 + 0.1 = 129.4	129.4	9.7	Ext
	119.4 - 1.6 + 1.7 - 0.7 = 118.8		128.4 + 9.0 + 1.2 - 9.2 = 129.4			
4	146.7 - 30.0 + (2.1 - 1.4) + 1.7 = 119.1	118.8	138.7 - 20.5 + 10.6 + 1.2 = 130.0	130.8	12.0	Ext
	116.2 - 1.6 + 2.1 + 1.7 = 118.4		141.8 - 20.5 + 9.0 + 1.2 = 131.5			
15	151.9 - 30.0 - 1.0 = 120.9	121.0	110.4 + 10.6 + 7.7 = 128.7	128.2	7.2	Med
	154.0 - 31.4 - 1.6 = 121.0		104.2 + 14.4 + 9.0 = 127.6			
16	150.8 - 30.0 - 1.6 = 119.2	119.2	109.2 + 10.6 + 9.0 = 128.8	128.8	9.6	Ext
17	149.0 - 30.0 + (2.1 - 1.4) - 1.6 = 118.1	119.0	129.2 - 20.5 + 10.6 + 9.0 = 128.3	128.4	9.4	Ext
	149.7 - 30.0 + 1.7 - 1.6 = 119.8		107.7 + 1.2 + 10.6 + 9.0 = 128.5			
18	147.6 - 30.0 + (2.1 - 1.4) + 1.7 - 1.6 = 118.4	118.4	127.2 - 20.5 + 1.2 + 10.6 + 9.0 = 127.5	127.5	9.1	Ext
19	156.1 - 31.4 - 1.0 = 123.7	123.7	104.0 + 14.4 + 7.7 = 126.1	126.1	2.4	Hin

Table 5

Theoretically calculated geometries (distances in Å, angles in °), total energies (in hartrees, ZPE corrected), relative energies (in kJ mol⁻¹) and dipole moments (in D). B3LYP/6-311++G(d,p) calculations. DIC conclusions from Table 4

Comp.	HB	d _{CN}	Torsion θ	Energy	Relative energy	Dipole
PhBzTr	—	1.428	0.00	-627.08073	—	0.34
1	Yes	1.426	0.00	-741.24756	—	1.60
2	Yes	1.431	0.04	-1016.23836	—	1.31
3	Yes	1.430	0.00	-1357.99068	0.00	1.93
3'	Yes	1.430	0.00	-1357.99064	0.08	0.98
4	Yes	1.430	0.00	-1475.84288	0.00	2.00
4'	Yes	1.430	0.00	-1475.84281	0.08	1.01
5	Yes	1.425	0.02	-780.53751	—	1.36
6	Weak	1.432	36.75	-780.52749	—	2.03
7	Weak	1.435	40.00	-937.66688	—	1.70
8	Weak	1.429	29.88	-816.45456	—	1.16
9	Weak	1.438	44.98	-1055.50679	—	1.61
10	Yes	1.426	0.00	-701.95738	—	1.64
11	Yes	1.427	0.00	-780.53852	—	1.07
12	Yes	1.430	0.00	-898.38652	—	1.27
13	Yes	1.427	0.00	-859.09971	—	1.63
14	Yes	1.430	0.00	-859.09638	—	1.40
15	Weak	1.425	34.19	-816.43484	—	1.94
16	Yes	1.423	0.00	-777.17461	—	3.03
17	Yes	1.427	0.00	-934.31296	—	3.05
18	Yes	1.431	0.00	-1091.45076	—	3.07
19	—	1.427	64.76	-855.69916	—	1.28

Table 6

Experimental geometries, DIC (degree of interannular conjugation) and number of IMHB (intramolecular hydrogen bonds)

Comp.	X-ray d _{CN}	X-ray θ	DIC	Number IMHB	O–H (Å)	H···N1 (Å)	OHN (°)
PhBzTr^a	1.432	1.1	Ext	0	—	—	—
1^b	1.430	1.4	Ext	1	1.00	1.767	142.7
2	—	—	—	1	—	—	—
3	—	—	Ext	1	—	—	—
4	1.423	12.7	Ext	1	1.09	1.57	153.9
5	—	—	—	1	—	—	—
6	—	—	—	1	—	—	—
7	1.437	89.3	—	1	c	c	c
8	—	—	—	1	—	—	—
9	—	—	—	1	—	—	—
10	—	—	—	1	—	—	—
11	—	—	—	1	—	—	—
12	1.427 ^d	5.3 ^d	—	1	0.81 ^d	1.84 ^d	151 ^d
	1.434 ^e	5.1 ^e	—	1	0.90 ^e	1.76 ^e	148 ^e
13	—	—	—	1	—	—	—
14	—	—	—	1	—	—	—
15	1.432	89.2 ^f	Med	1	0.98	1.94	172.0
16	1.434	4.4	Ext	2	1.07	1.82	126.5
17	—	—	Ext	2	—	—	—
18	1.432	0	Ext	2	1.08	1.55	152.6
					1.04	1.61	146.3
19	1.429	86.5	Hin	0	—	—	—
	1.431	86.6					

^a X-ray, from Ref. 4d.

^b X-ray, from Ref. 4b.

^c No IMHB.⁶

^d From Ref. 6.

^e From Ref. 10.

^f Hydrate (this work).

involved in the IMHB with two correcting terms. If two OH groups (**16**, **17**, **18**) or two methoxy groups (**19**) are present $\cos^2\theta$ decreases by approximately the same amount, that is, these compounds are less planar than will be expected from the chemical shift of N1.

$$\cos^2\theta = -(0.33 \pm 0.04) - (0.0178 \pm 0.0005)\delta^{15}\text{N calc. N1} \\ - (0.40 \pm 0.02)[2 \text{ OH}] - (0.48 \pm 0.00)[2 \text{ OCH}_3], \\ n = 20, R^2 = 0.994 \quad (3)$$

Statistically, in the solid-state structure **3** fits better than **3'** and structure **4** better than **4'**, therefore they are 5-chloro and not 6-chloroderivatives (Fig. 13). Compounds **3'** and **4'** were not used for calculated Eqs. 2 and 3. In solution, the data corresponds to a ~50/50 mixture of **3** and **3'** and **4** and **4'**. The ¹⁵N chemical shifts are sensitive to the buttressing effect:¹⁷ for instance the ^tBu group pushes the OH toward N1. Considering the N1 and N3 chemical shifts, we observed that in compound **16** (no ^t-Bu) they resonate at -96.6 ppm; in compound **18** (two ^t-Bu) at -98.6 ppm, finally, in compound **17** (one ^t-Bu) at -98.8 ppm (near the ^t-Bu) and -96.6 ppm (far from the ^t-Bu).

To establish relationships similar to those of Table 4 it is necessary to correct the calculated ¹³C chemical shifts of the positions *ortho* and *meta* (2'/3' and 6'/5') for the substituent effects. To avoid this semi-empirical approach, we have used the calculated ¹⁵N chemical shifts of N3 (usually not involved in the O–H···N IMHB). The equation needs a term for compounds **16–18** where N3 has also an IMHB and another for compound **19** that has no IMHB.

Using the 2-phenylbenzotriazole (**PhBzTr**) as a model we have calculated the chemical shifts of the *meta* and *ortho* carbons as a function of the dihedral angle θ. The difference, Δδ, was plotted against θ and the calculated points roughly correspond to Eq. 4 and Fig. 14.

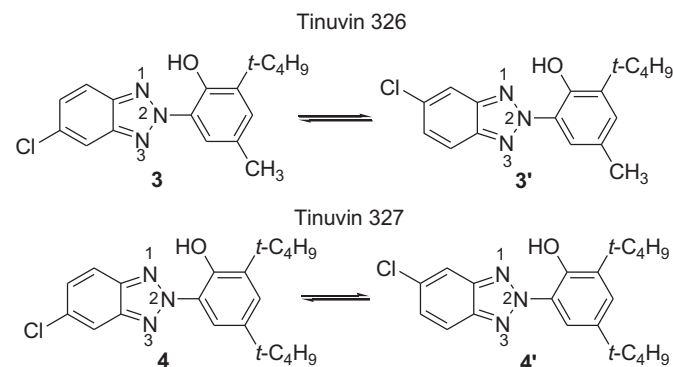


Fig. 13. The two conformations of Tinuvin 326 and Tinuvin 327.

experimental value of the ¹H chemical shift of the OH group (measured only in solution) but that a corrective term should be added when there is an O–H···N IMHB. Note that the intercept is not significant.

$$\delta^1\text{H OH exp.} = (1.1 \pm 2.0) + (0.75 \pm 0.20)\delta^1\text{H calc.} \\ + (1.76 \pm 0.41) \text{ IMHB}, \\ n = 10, R^2 = 0.971 \quad (1)$$

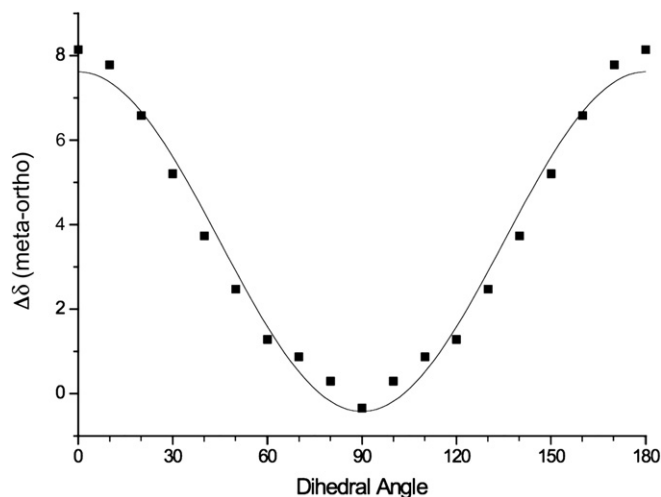
Eq. 2 corresponds to all available data, both in solution and in the solid state. There is a significant intercept because the empirical equation to transform σ into δ uses ¹⁵N chemical shifts from a large variety of compounds while here the range is quite small (between -49.4 and -114.9 ppm). The presence of HBs that affect N1 and N3 (but not N2) needs a rather important term (12.6 ppm).

$$\delta^{15}\text{N exp.} = -(15.2 \pm 4.4) + (0.89 \pm 0.04)\delta^{15}\text{N calc.} \\ + (12.6 \pm 0.9) \text{ N1} + \text{N3}, \\ n = 33, R^2 = 0.985 \quad (2)$$

Finally, Eq. 3 shows that the torsion transformed into $\cos^2\theta$ (but when $\cos^2\theta$ increases so do θ) depends on the N atom

Table 7Some relevant calculated chemical shifts of the *ortho*-hydroxy derivatives **1–18** together with some experimental data in solution and in the solid state

Comp.	¹⁵ N1 (HB)	¹⁵ N2	¹⁵ N3	Average N1/N3	¹⁷ O	¹ H OH	Solution N1/N3	Solution N2	Solution OH	Solid N1	Solid N2	Solid N3
1 ^a	−95.4	−106.9	−75.0	−85.2	77.9	11.16	−80.1	−110.1	11.10	−89.3	−107.3	−69.7
2	−97.7	−105.3	−74.5	−86.1	83.5	12.14						
3	−97.2	−103.8	−75.7	−86.4	83.5	11.88				−87.6	−105.1	−67.9
3'	−99.1	−104.1	−74.0	−86.6	83.6	11.88				−87.6	−105.1	−67.9
3/3'	−98.2	−104.0	−74.8	−86.5	83.6	11.88	−80.9 −78.9	−106.6	11.47			
4	−97.3	−103.1	−76.1	−87.6	83.4	11.90				−86.7	−103.8	−66.8
4'	−99.2	−103.4	−74.4	−86.8	83.5	11.91				−86.7	−103.8	−66.8
4/4'	−98.2	−103.2	−75.2	−87.2	83.4	11.90	−80.8 −78.6	−105.6	11.53			
5	−96.0	−106.5	−76.0	−86.0	77.6	11.09			11.04 ^b			
6	−81.3	−110.1	−53.9	−67.6	62.4	9.64			8.04 ^b			
7	−81.3	−109.7	−51.9	−66.6	64.3	10.05						
8	−88.5	−108.8	−60.1	−74.3	72.5	10.74						
9	−77.2	−110.2	−49.4	−63.3	61.5	9.26						
10	−95.4	−107.4	−74.7	−85.0	81.3	11.34						
11	−96.1	−106.4	−74.5	−85.3	77.8	11.47						
12	−97.8	−105.9	−74.3	−86.0	83.5	12.10						
13	−95.4	−106.2	−75.3	−85.4	78.0	11.18						
14	−97.7	−106.3	−74.0	−85.8	86.8	12.25						
15	−85.2	−114.9	−55.2	−70.2	68.0	10.03	−65.5	n.d.	8.93		—	
16	−96.6	−104.8	−96.6	−96.6	82.1	11.33	−87.7	−110.9	11.45	−89.6	−106.5	−89.6
17	−98.8 ^c	−104.0	−96.6	−97.7	88.4 ^c	12.24 ^c	−87.8	−109.9	12.12 ^c	−89.2	−107.1	−89.2
					79.8	11.30			11.34			
18	−98.6	−103.1	−98.6	−98.6	86.3	12.25	−87.5	−109.2	11.90	−90.0	−108.9	−90.0

^a From Ref. 4d.^b From Ref. 6.^c Near the *t*-Bu.**Fig. 14.** Variation of $\Delta\delta$ in function of the torsion angle θ in **PhBzTr**. GIAO/B3LYP/6-311++G(d,p) calculations.

$$\Delta\delta = -(0.42 \pm 0.17) + (8.04 \pm 0.27)\cos^2\theta, \quad (4)$$

$$n = 19, R^2 = 0.98$$

In its ground state, the molecule is planar, $\theta=0^\circ$, and to this conformation corresponds $\Delta\delta=8.14$ ppm that compare well with the experimental value of 8.8 ppm (Table 4). The conformation $\theta=90^\circ$ is the transition state (19.0 kJ mol^{−1} including the zero-point error correction) where $\Delta\delta=-0.35$ ppm.

This curve shows that $\Delta\delta$ is sensitive enough to determine the torsion angle in 2-aryl-benzotriazoles with enough precision for our purpose. The average $\Delta\delta$ value of Table 4 for $\theta=0^\circ$ is 9.8 ppm,

i.e., 1.2 larger than the calculated for **PhBzTr** (note that the substituents modify the geometry, for instance the interring N–C distance). In the case of non-planar compounds **15** ($\theta=34.2^\circ$) and **19** ($\theta=64.8^\circ$) the Eq. 4 predicts 5.1 ppm and 1.0 ppm, respectively, lower than 7.2 ppm (ratio 7.2/5.1=1.4) and 2.4 ppm (ratio 2.4/1.0=2.4), but still acceptable considering all the approximations involved.

3. Conclusions

The study of the molecular structure of a large collection of Tinuvin has been carried out. The behavior of these compounds is mutually consistent proving that theoretical calculations for the gas phase (isolated molecules) can be used to predict the molecular properties of their ground states. Even subtle differences like those existing between **3** and **3'** and between **4** and **4'** can be determined theoretically agreeing with the experimental results.

4. Experimental

4.1. General

Melting points were determined with a ThermoGalen hot stage microscope and are given uncorrected. Elemental analyses for carbon, hydrogen, and nitrogen were performed by the Microanalytical Service of the Complutensian University of Madrid, using a Perkin–Elmer 240 analyzer. Column chromatography was conducted on silica gel (Merck 60, 70–230 mesh). *R_f* values were measured on aluminum-backed TLC plates of silica gel 60 F₂₅₄ (Merck, 0.2 mm) with the indicated eluent.

Tinuvin 326 (**3**) and Tinuvin 327 (**4**) are commercial products from Aldrich and were used without further purification. Benzotriazoles **16** and **19** are known compounds and were prepared according to the literature using the procedure described by Evans,⁷ with yields of 85% and 73%, respectively.

4.1.1. 2-(2-Hydroxy-6-methoxy)-2H-benzotriazole (15). A mixture of 1.135 g (5 mmol) of 2-(2,6-dihydroxy)-2H-benzotriazole (**16**), 0.288 g (7.2 mmol) of NaOH in 20 mL of water, and 20 mL of toluene was heated up to 100 °C. Then a solution of 0.665 g (5.27 mmol) of Me₂SO₄ in 30 mL of toluene was added at a rate of 12–15 drops per min. A vigorous stirring was needed during the addition process that takes about 1.5 h. Afterward, 0.3 g of NaOH in 30 mL of water were added and the reaction mixture stirred, the alkaline aqueous phase was separated and acidified to pH 6, with diluted HCl affording a precipitate that was filtered and washed with water. The crude product thus isolated was purified by column chromatography on Merck silica gel 60 with chloroform as eluent. The first fraction contained 0.22 g of the starting material (*R_f*: 0.56, chloroform), and the second one 0.25 g (19.7% yield) of **15**, *R_f*: 0.15, chloroform. Mp: 155–156 °C (ethanol). Anal. Calcd for C₁₃H₁₁N₃O₂ (241.25): C, 64.72; H, 4.60; N, 17.42; found: C, 65.03; H, 4.54; N, 17.0%.

4.1.2. 2-(2,6-Dihydroxy-3-tert-butylphenyl)-2H-benzotriazole (17). To achieve the reaction, dryness conditions all through the procedure must be maintained: a mixture of 0.454 g (2 mmol) of 2-(2,6-dihydroxy)-2H-benzotriazole (**16**) dried under vacuum at 60 °C, 0.5 g (3.6 mmol) of dry finely powdered K₂CO₃, 0.822 g (6 mmol) of *tert*-butyl bromide and 1 g of Merck silica gel 60 previously activated for 5 h under vacuum at 190 °C, and 15 mL of carbon tetrachloride freshly distilled and dried over 4 Å molecular sieves, was heated at 70–73 °C with vigorous stirring during 24 h. The reaction mixture was filtered at such temperature and after thorough washing of the solid materials with dichloromethane, all organic washings were joined to the filtrate and the solvent evaporated off under reduced pressure. The crude residue was then purified by column chromatography on Merck silica gel 60 with hexane/chloroform (6:4) as eluent. *R_f*=0.48 (hexane/chloroform 6:4). Thus compound **17** was obtained, 0.25 g (44.2% yield). Mp: 187–189 °C (cyclohexane). Anal. Calcd for C₁₆H₁₇N₃O₂ (283.33): C, 67.83; H, 6.05; N, 14.83; found: C, 67.44; H, 6.12; N, 14.58%. Unreacted starting material **16** and traces of **18** were also isolated.

4.1.3. 2-(2,6-Dihydroxy-3,5-di-tert-butylphenyl)-2H-benzotriazole (18). To achieve this reaction dryness conditions all through the procedure must be maintained: a mixture of 0.454 g (2 mmol) of 2-(2,6-dihydroxy)-2H-benzotriazole dried under vacuum at 60 °C, 0.5 g (3.6 mmol) of dry finely powdered K₂CO₃, 2.46 g (18 mmol) of *tert*-butyl bromide and 1.5 g of Merck silica gel 60 previously activated for 5 h under vacuum at 190 °C, and 12 mL of carbon tetrachloride freshly distilled and dried over 4 Å molecular sieves, was heated at 70–73 °C with vigorous stirring during 40 h. The reaction mixture was filtered at such temperature and after thorough washing of the solid materials with dichloromethane, all organic washings were joined to the filtrate and the solvent evaporated off under reduced pressure. The crude residue was purified by column chromatography on Merck silica gel 60 with hexane/chloroform (6:4) as eluent. *R_f*=0.81 (hexane/chloroform 6:4). The entitled compound **18** was obtained, 0.55 g (81.0% yield). Mp: 203–204 °C (cyclohexane). Lit. (Ciba-Geigy):¹⁸ 211 °C (petroleum ether). Traces of **17** (5.6% yield) were also isolated.

4.2. NMR spectroscopy

Solution NMR spectra were recorded on a Bruker DRX 400 (9.4 T, 400.13 MHz for ¹H, 100.62 MHz for ¹³C and 40.56 MHz for ¹⁵N) spectrometer with a 5-mm inverse-detection H-X probe equipped with a *z*-gradient coil. Chemical shifts (δ in parts per

million) are given from internal solvent, CDCl₃, 7.26 for ¹H and 77.0 for ¹³C; for ¹⁵N NMR nitromethane (0.00) was used as external standard. 2D (¹H–¹H) *gs*-COSY and inverse proton detected heteronuclear shift correlation spectra, (¹H–¹³C) *gs*-HMBC, (¹H–¹³C) *gs*-HMBC and (¹H–¹⁵N) *gs*-HMBC, were carried out with the standard pulse sequences¹⁹ to assign the ¹H, ¹³C and ¹⁵N signals. 1D ¹⁵N NMR spectra were obtained with inverse gated ¹H decoupling technique.

Solid-state ¹³C (100.73 MHz) and ¹⁵N (40.60 MHz) CPMAS NMR spectra were obtained on a Bruker WB 400 spectrometer at 300 K using a 4 mm DVT probehead. Samples were carefully packed in a 4-mm diameter cylindrical zirconia rotor with Kel-F end-caps. ¹³C spectra were originally referenced to a glycine sample and then the chemical shifts were recalculated to the Me₄Si (for the carbonyl atom δ (glycine)=176.1 ppm) and ¹⁵N spectra to ¹⁵NH₄Cl and then converted to nitromethane scale using the relationship: δ ¹⁵N(nitromethane)= δ ¹⁵N(ammonium chloride)–338.1 ppm. The typical acquisition parameters for ¹³C CPMAS were: spectral width, 40 kHz; recycle delay, 5 s (75 s for **16**); acquisition time, 39 ms; contact time, 2 ms; and spin rate, 12 kHz. In order to distinguish protonated and unprotonated carbon atoms, the NQS (Non-Quaternary Suppression) experiment by conventional cross-polarization was recorded; before the acquisition the decoupler is switched off for a very short time of 25 μ s. The typical acquisition parameters for ¹⁵N CPMAS were: spectral width, 29 kHz; recycle delay, 5 s (75 s for **16**); acquisition time, 35 ms; contact time, 6–9 ms; and spin rate, 6 kHz.

4.3. Computational details

Optimization and frequency calculations were carried out at the B3LYP^{20–22}/6-31G(d) level,²³ optimization and GIAO calculations^{24,25} were carried out at the B3LYP/6-311++G(d,p) level,^{26,27} total (hartree) and relative (kJ mol⁻¹) energies correspond to B3LYP/6-311++G(d,p) calculations. The Gaussian 09 package was used for all the calculations.²⁸

4.3.1. X-ray data collection and structure refinement. Data collection for all compounds were carried out at room temperature on a Bruker Smart CCD diffractometer using graphite-monochromated Mo-K α radiation (λ =0.71073 Å) operating at 50 kV and 35 mA for **15**, **16**, and **18**, 30 mA for **4** and 25 mA for **19**. In all cases, the data were collected over a hemisphere of the reciprocal space by combination of three exposure sets; each exposure was of 20 and covered 0.3° in ω . The first 100 frames were recollected at the end of the data collection to monitor crystal decay, and no appreciable decay was observed in all the cases. A summary of the fundamental crystal and refinement data is given in Table 8.

The structures were solved by direct methods and refined by full-matrix least-square procedures on *F*² (SHELXL-97).²⁹ All non-hydrogen atoms were refined anisotropically. All hydrogen atoms were included in calculated positions and refined riding on the respective carbon atoms, with some exceptions concerning the hydroxyl groups. Thus, H1 and H3A for **15**, H1 for **16** and H1 and H2 for **18** were located in a Fourier synthesis map and refined riding on the respective oxygen bonded atoms.

In compound **4** one of the *tert*-butyl groups is disordered over two sites with 0.63:0.37 occupancies. The phenol group is also disordered on C9 (O1 with 80% occupancy) and on C13 (O1' with 20% occupancy). The hydrogen atom, H1, bonded to O1, was located in a Fourier synthesis map and refined riding on O1, while the hydrogen atom bonded to O1' was not located.

Table 8
Crystal data and structure refinement for benzotriazoles **4**, **15**, **16**, **18**, and **19**

Crystal data	4	15	16	18	19
Identification code	CCDC-905042	CCDC-905043	CCDC-905044	CCDC-905045	CCDC-905046
Empirical formula	C ₂₀ H ₂₄ ClN ₃ O	C ₁₃ H ₁₃ N ₃ O ₃	C ₁₂ H ₉ N ₃ O ₂	C ₂₀ H ₂₅ N ₃ O ₂	C ₁₄ H ₁₃ N ₃ O ₂
Formula weight	357.87	259.26	227.22	339.43	255.27
Crystal system	Triclinic	Orthorhombic	Orthorhombic	Monoclinic	Orthorhombic
Space group	<i>P</i> -1	<i>Pnma</i>	<i>Pnma</i>	<i>P2</i> ₁ / <i>m</i>	<i>Iba</i> 2
<i>Unit cell dimensions</i>					
<i>a</i> (Å)	6.043(2)	23.125(2)	22.392(11)	9.789(2)	19.676(1)
<i>b</i> (Å)	9.866(3)	7.0626(7)	11.872(4)	6.874(1)	19.677(1)
<i>c</i> (Å)	16.089(5)	7.9896(8)	3.800(2)	14.267(3)	13.790(1)
α (°)	86.000(6)	—	—	—	—
β (°)	88.945(6)	—	—	102.038(3)	—
γ (°)	82.472(6)	—	—	—	—
Volume (Å ³)	948.6(5)	1304.9(2)	1010.1(7)	939.0(3)	5339.1(7)
<i>Z</i>	2	4	4	2	16
Density (calculated) (Mg/m ³)	1.253	1.320	1.494	1.201	1.270
Absorption coefficient (mm ⁻¹)	0.214	0.096	0.106	0.079	0.088
<i>F</i> (000)	380	544	472	364	2144
Theta range (°) for data collection	1.27 to 25.00	1.76 to 26.99	1.82 to 27.00	1.46 to 26.00	1.46 to 26.99
Index ranges	−7 ≤ <i>h</i> ≤ 7 −11 ≤ <i>k</i> ≤ 9 −19 ≤ <i>l</i> ≤ 19	−29 ≤ <i>h</i> ≤ 26 −9 ≤ <i>k</i> ≤ 8 −10 ≤ <i>l</i> ≤ 10	−28 ≤ <i>h</i> ≤ 28 −11 ≤ <i>k</i> ≤ 15 −4 ≤ <i>l</i> ≤ 4	−12 ≤ <i>h</i> ≤ 10 −8 ≤ <i>k</i> ≤ 8 −17 ≤ <i>l</i> ≤ 17	−25 ≤ <i>h</i> ≤ 25 −23 ≤ <i>k</i> ≤ 25 −16 ≤ <i>l</i> ≤ 17
Reflections collected	6873	11,070	7784	7772	23,251
Independent reflc. [<i>R</i> (int)]	3224 [0.1097]	1536 [0.0510]	1145 [0.1296]	1999 [0.0501]	5702 [0.0575]
Completeness to theta (%)	96.5	100	99.7	99.5	99.9
Data/restraints/parameters	3224/10/264	1536/0/103	1145/0/82	1999/4/145	5702/1/343
Goodness-of-fit on <i>F</i> ²	0.996	0.992	0.997	0.994	0.998
<i>R</i> 1 (reflns obsd) [<i>I</i> > 2σ(<i>I</i>)] ^a	0.0565 (2006)	0.0396 (786)	0.0466 (565)	0.0438 (900)	0.0397 (3028)
<i>wR</i> 2 (all data) ^b	0.1706	0.1277	0.1619	0.1235	0.0924

^a $R1 = \sum ||F_o| - |F_c|| / \sum |F_o|$.

^b $wR2 = \{ \sum [w(F_o^2 - F_c^2)]^2 / \sum [w(F_o^2)]^2 \}^{1/2}$.

Acknowledgements

This work has been financed by the Spanish MICINN (CTQ2009-13129-C02-02 and CTQ2010-16122) and Comunidad Autónoma de Madrid (Project MADRISOLAR2, ref S2009/PPQ-1533). The authors thank the CTI (CSIC) for allocation of computer time.

Supplementary data

NMR and computational details, CIFs and Checkcif, associated with this article can be found in the online version. Supplementary data related to this article can be found at <http://dx.doi.org/10.1016/j.tet.2013.01.096>.

References and notes

- (a) Tinuvin P is a Trademark of Ciba-Geigy Ltd, The First Patent is from 14.12.1956 (Fr. Pat. 1.195.207), 1960. (b) Chemical Information Review Document for Phenolic Benzotriazoles; National Toxicology Program: October 2011; <http://ntp.niehs.nih.gov/>.
- Half of Sun Products have BASF UV Filters; Chemistry World, Royal Society of Chemistry: March 2012.
- (a) Kirkbright, G. F.; Narayanaswamy, R.; West, T. S. *Anal. Chim. Acta* **1970**, *52*, 237–246; (b) Otterstedt, J.-E. A. *J. Chem. Phys.* **1973**, *58*, 5716–5725; (c) Heller, H. J.; Blattmann, H. R. *Pure Appl. Chem.* **1973**, *141*–161; (d) Paul, B. K.; Guchhait, N. *Comput. Theor. Chem.* **2011**, *966*, 250–258.
- (a) Catalán, J.; Pérez, P.; Fabero, F.; Wilshire, J. F. K.; Claramunt, R. M.; Elguero, J. *J. Am. Chem. Soc.* **1992**, *114*, 964–966; (b) Catalán, J.; de Paz, J. L. G.; Torres, M. R.; Tornero, J. D. *J. Chem. Soc., Faraday Trans.* **1997**, *93*, 1691–1696; (c) Catalán, J.; Pérez, P.; Claramunt, R. M.; Santa María, D.; Bobosik, V. *Chem. Phys.* **2007**, *340*, 32–42; (d) Claramunt, R. M.; Santa María, D.; Pinilla, E.; Torres, M. R.; Elguero, J. *Molecules* **2007**, *12*, 2201–2214.
- (a) Maliakal, A.; Lem, G.; Turro, N. J.; Ravichandran, R.; Suhadolnik, J. C.; DeBellis, A. D.; Wood, M. G.; Lau, J. *J. Phys. Chem. A* **2002**, *106*, 7680–7689; (b) Paterson, M. J.; Robb, M. A.; Blancfort, L.; DeBellis, A. D. *J. Am. Chem. Soc.* **2004**, *126*, 2912–2922; (c) Xu, X.-F.; Gao, F.; Li, H.-R.; Zhang, S.-T. *Acta Phys.-Chim. Sin.* **2010**, *26*, 131–140; (d) Farkas, R.; Lhiaubet-Vallet, V.; Corbera, J.; Tórcin, M.; Gorchs, O.; Trullas, C.; Jiménez, O.; Miranda, M. A.; Novak, L. *Molecules* **2010**, *15*, 6205–6216; (e) Li, H.; Niu, L.; Xu, X.; Zhang, S.; Gao, F. *J. Fluoresc.* **2011**, *21*, 1721–1728; (f) Ma, J.; Zhao, J.; Yang, P.; Huang, D.; Zhang, C.; Li, Q. *Chem. Commun.* **2012**, 9720–9722.
- Rieker, J.; Lemmert-Schmitt, E.; Goeller, G.; Roessler, M.; Stueber, G. J.; Schettler, H.; Kramer, H. E. A.; Stezowski, J. J.; Holzer, H.; Henkel, S.; Schmidt, A.; Port, H.; Wiechmann, M.; Rody, J.; Rytz, G.; Slongo, M.; Birbaum, J.-L. *J. Phys. Chem.* **1992**, *96*, 10225–10234.
- Evans, N. E. *Aust. J. Chem.* **1981**, *34*, 691–695.
- Liu, G.-B.; Zhao, H.-Y.; Yang, H.-J.; Gao, X.; Li, M.-K.; Thiemann, T. *Adv. Synth. Catal.* **2007**, *349*, 1637–1640.
- Rosevear, J.; Wilshire, J. F. K. *Aust. J. Chem.* **1982**, *35*, 2089–2093.
- Greenwood, R. J.; Mackay, M. F.; Wilshire, J. F. K. *Aust. J. Chem.* **1992**, *45*, 965–968.
- Heller, H. J. *Eur. Polym. J. (Suppl.)* **1969**, 105–132.
- Cambridge Structural Database Allen, F. H. *Acta Crystallogr., Sect. B* **2002**, *58*, 380–388; Allen, F. H.; Motherwell, W. D. S. *Acta Crystallogr., Sect. B* **2002**, *58*, 407–422 CSD Version 5.32, updated Feb. 2011; <http://www.ccdc.cam.ac.uk>.
- Woessner, G.; Goeller, G.; Kollat, P.; Stezowski, J. J.; Hauser, M.; Klein, U. K. A.; Kramer, E. A. *J. Phys. Chem.* **1984**, *88*, 5544–5550.
- Kamitori, Y.; Hojo, M.; Masuda, R.; Izumi, T.; Tsukamoto, S. *J. Org. Chem.* **1984**, *49*, 4161–4165.
- (a) Houghton, P. G.; Pipe, D. F.; Rees, C. W. *J. Chem. Soc., Chem. Commun.* **1979**, 771–772; (b) Houghton, P. G.; Pipe, D. F.; Rees, C. W. *J. Chem. Soc., Perkin Trans. 1* **1985**, 1471–1479.
- Kalinowski, H. O.; Berger, S.; Braun, S. *Carbon-13 NMR Spectroscopy*; John Wiley & Sons: Chichester, UK, 1988; p 313.
- (a) Trofimenko, S.; Rheingold, A. L.; Liable-Sands, L. M.; Claramunt, R. M.; López, C.; Santa María, M. D.; Elguero, J. *New J. Chem.* **2001**, *25*, 819–823; (b) Alkorta, I.; Elguero, J.; Roussel, C.; Vanthuyne, N.; Piras, P. *Adv. Heterocycl. Chem.* **2012**, *105*, 1–188.
- Heller, H. J. Ciba-Geigy. Personal communication.
- Berger, S.; Braun, S. *200 and More Basic NMR Experiments*; Wiley-VCH: New York, NY, 2004.
- Becke, A. D. *Phys. Rev. A: At., Mol., Opt. Phys.* **1988**, *38*, 3098–3100.
- Becke, A. D. *J. Chem. Phys.* **1993**, *98*, 5648–5652.
- Lee, C.; Yang, W.; Parr, R. G. *Phys. Rev. B: Condens. Matter* **1988**, *37*, 785–789.
- Hariharan, P. A.; Pople, J. A. *Theor. Chim. Acta* **1973**, *28*, 213–222.
- Ditchfield, R. *Mol. Phys.* **1974**, *27*, 789–807.
- London, F. J. *Phys. Radium* **1937**, *8*, 397–409.
- Ditchfield, R.; Hehre, W. J.; Pople, J. A. *J. Chem. Phys.* **1971**, *54*, 724–728.
- Frisch, M. J.; Pople, J. A.; Binkley, J. S. *J. Chem. Phys.* **1984**, *80*, 3265–3269.
- Frisch, M. J.; Trucks, G. W.; Schlegel, H. B.; Scuseria, G. E.; Robb, M. A.; Cheeseman, J. R.; Scalmani, G.; Barone, V.; Mennucci, B.; Petersson, G. A.; Nakatsuji, H.; Caricato, M.; Li, X.; Hratchian, H. P.; Izmaylov, A. F.; Bloino, J.; Zheng, G.; Sonnenberg, J. L.; Hada, M.; Ehara, M.; Toyota, K.; Fukuda, R.; Hasegawa, J.; Ishida, M.; Nakajima, T.; Honda, Y.; Kitao, O.; Nakai, H.; Vreven, T.; Montgomery, J. A., Jr.; Peralta, J. E.; Ogliaro, F.; Bearpark, M.; Heyd, J. J.; Brothers, E.; Kudin, K. N.; Staroverov, V. N.; Kobayashi, R.; Normand, J.; Raghavachari, K.; Rendell, A.; Burant, J. C.; Iyengar, S. S.; Tomasi, J.; Cossi, M.; Rega, N.; Millam, N. J.; Klene, M.;

Knox, J. E.; Cross, J. B.; Bakken, V.; Adamo, C.; Jaramillo, J.; Gomperts, R.; Stratmann, R. E.; Yazyev, O.; Austin, A. J.; Cammi, R.; Pomelli, C.; Ochterski, J. W.; Martin, R. L.; Morokuma, K.; Zakrzewski, V. G.; Voth, G. A.; Salvador, P.; Dannenberg, J. J.; Dapprich, S.; Daniels, A. D.; Farkas, Ö.; Foresman, J. B.; Ortiz, J. V.;

Cioslowski, J.; Fox, D. J. *Gaussian 09, Revision A.1*; Gaussian: Wallingford CT, 2009.

29. Sheldrick, G. M. *SHELX97, Program for Refinement of Crystal Structure*; University of Göttingen: Göttingen, Germany, 1997.